Journal of Engineering and Applied Sciences 12 (15): 3818-3823, 2017
ISSN: 1816-949X

Positioning of Fused Deposition Features on Primitives

Patharawut Suphama, Kuntinee Maneeratana and Ratchatin Chancharoen
Department of Mechanical Engineering, Faculty of Engineering,
Chulalongkorn University, Bangkok, Thailand

Abstract: This study proposed a technique for constructing 3D features on top of primitive objects by Fused Deposition Modeling (FDM). The arduino-driven platform was based on a fast and stiff linear Delta robot with a close-loop control and incorporated FDM technology. The print head navigated with a camera with real-time feature extraction algorithm to determine the position and orientation of the printed feature with respect to the geometry of the primitive object. Minimal or no fixture for the primitive object was required, depending on the bed-primitive interface friction. With the naturally 3D motion of Delta robots, features could be constructed layer by layer on top of the leveled or inclined plastic-base commercial products at the same cost. This concept combined the Additive Manufacturing (AM), positioning and assembly into a single process with high energy, cost and time saving potentials.

Key words: 3D printer, visual positioning, Delta robot, close-loop control, arduino

INTRODUCTION

Fused Deposition Modeling (FDM), commonly called 3D Printing or 3DP (Evans, 2012) was a rapid prototyping system that produced 3D features by using thermoplastic extruders to melt and lay tracks of quasi-liquid plastic filaments layers by layers with infill patterns for solid bodies on the build platform or print bed in to the desired geometry from bottom to the top.

One of the problems encountered in the printing process of a component was the warping of feature as the molten plastic cooled down rapidly and started shrinking. This phenomenon not only caused the geometry inaccuracy but also the detachment of the printing feature from the print bed which caused printing failure. Many print platforms in the market countered this problem by using heat print beds on which the plastic slowly cooled down and created better adhesion between the first layer and the print platform (Evans, 2012**)**. Other solutions from commercial printer providers included the use of acetone to treat printing surface in order to promote the bonding with ABS or the perf board print bed on which the perforation increased the interference strength. Some recommended the application of the Kapton tape, blue painter's tape or glue, depending on the type of plastic filaments. Another response was the use of raft structure in which the printer first printed an evenly spaced platform on which the features were produced. The raft, removed from the feature afterwards, reduced surface irregularities in the build platform during the manufacture and aids the part separation from the bed.

In short, it was clear that during the manufacturing, the first few layers of the 3D features had to be well-stuck to the print platform and then had to be detached gently afterwards. With the temperature of the molten plastic of around 170-220°C it was likely that they could easily stick to surfaces of many products. Hence, this study proposed that instead of producing separated components that had to be assembled again in many cases it would be more expedient to print the 3D features onto a base component or even commercial products instead.

To prove the concept, 3 main areas had to be considered. First, the printer head had to be able to be repositioned with respect to the dimension of the primitive object by either manual or visual-based algorithm. Secondly, the printer had to be able to adjust the height in the z-axis of the printing head so that the crucial first few layers would be printed on the surface that was not flatly aligned to the generally x-y printing plane the first few layers were critical since the built material might not firmly sit down on the surface if the printing head was too far way or spread out if it was too close. This first layer situation somewhat resembled bonding strength between the soldering and the board in the direct printing of electrical circuit (Kim *et al*., 2009). Lastly, the printed featured had to have satisfactory bonding strength with the primitive base.

The object of this study was to test the adaptation of a 3D printer for the printing on the desired position with the aid of camera to determine the location accurately. The effect of the printing plane that is inclined was also considered.

Corresponding Author: Ratchatin Chancharoen, Department of Mechanical Engineering, Faculty of Engineering, Chulalongkorn University, Bangkok, Thailand

MATERIALS AND METHODS

The linear delta robot: A Delta robot consisted of three parallel mechanisms to constrain the end effector such that it was parallel to the base at all time and thus promised the alignment of the print head to the gravity field. The Delta robot both revolute and linear types had drawn much attention in the past two decades due to their relative advantages including high stiffness, high accuracy and low moving inertia at the expense of more complex kinematics, less work space and interference between joints (Yiu, 2002).

In the project a Delta robot was custom designed and built to move a print head in 3-Dimensional space. The linear type robot was chosen due to a higher stiffness in this application due to the strength requirement to overcome the accumulate deposition and in-plane position errors in the built process. The close loop control system also enhanced the deposition and position accuracy.

The designed Delta robot, CHULA DELTA 3D PRINTER R100 was driven by three PMDC motors, each equipped with with 64:1 planetary gear and 12-PPR encoder. Linear guides with belt drives were used to transmit the force and motion to the 3D printed end effector since they offered good precision at a relatively low cost (Cunico and Carvalho, 2013). Two laser cut acrylic plates were used to fix the linear guides in position as shown in Fig. 1.

When a feature was to be built on top of a primitive or functional products using FDM technique, the proposed stiff linear Delta robot would probe a surface and move the print head in three dimensional space to maintain the nozzle's distance. This ensured that the first layer was perfectly laid on the surface even the platform was not in good leveling or on an incline surface. The resulting bottom surface of the built feature would be compatible with the surface that it was built on and ensured a good fit as molten plastic exited the nozzle, cooled down and formed its track even when the built surface is not flat.

Processing system: The processing system combined the power of x64 processor and FPGA with low cost arduino board to process heavy floating point mathematics at 1 msec realtime servo rate while all safety switches were monitored at all time. The computing system consisted of 2 computers, 1 FPGA and two arduino MEGA 2560 boards. The host computer was windows based which interfaces to all the USB devices and both Arduino boards and the realtime computer. The realtime computer ran the control loop and communicated with FPGA at

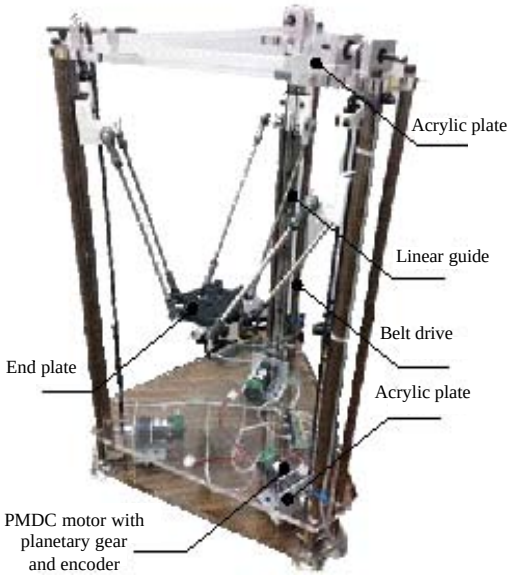

Fig. 1: The custom Delta robot

1 kHz servoing rate. The FPGA commanded motor drivers, processed encoder signals and handled all switches in the robot and the manual pulse generator. One Arduino board was loaded with 3D printer firmware and plugged with 3D printer electronics while the other board was to be general purpose I/Os including analog to the system. The processing system was reconfigurable and specially designed for a research robotics system. The major reconfigurable characteristics include modularity, integrability, customization and diagnosibility (Dashchenko, 2006) which were keys to enable new techniques and strategies to the 3D printer.

The Delta robot's closed loop position control used encoders as feedback sensors. The Inverse Kinematics (IK) mapped the cartesian position reference into three joint references which were fed to the joint controllers. The PID (Dorf and Bishop, 1998) controller received the joint references and processed three joint servo loops simultaneously at 1 kHz to control all joints to follow their references. The PWM (Alciatore, 2007) motor driver circuits were also updated at this rate. The encoder module in FPGA is 16 bit wide where the encoder's counter is increased to 32 bit wide in the realtime computer. The resolution of the PWM is 14 bit. There was a software switch for selecting the Cartesian reference input between 3 options, 3D printer software, manual pulse generator or built in trajectory.

Robot performance: The performance of the joint controller was demonstrated in two control performance in joint and cartesian spaces.

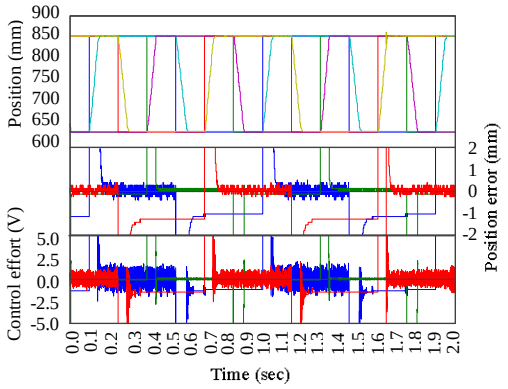

Fig. 2: Simultaneous step response

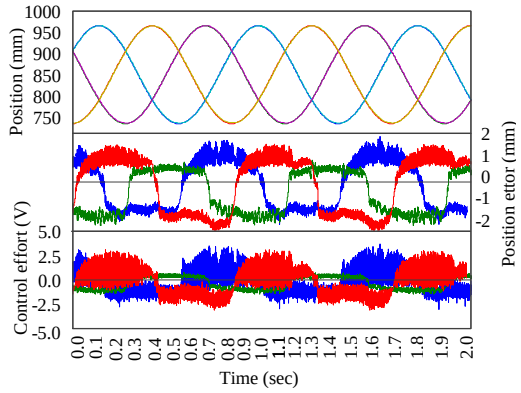

Fig. 3: Response for an in-plane circular trajectory

Simultaneous step responses in joint space: In this experiment, the three joints were commanded to track 200 mm step reference with 900 m sec interval and 300 msec delay. The time constant was approximated at 0.05 sec while the steady state error was within 0.3 mm. The result in Fig. 2 and 3 demonstrated that there was less interference between joints in control performance.

Tracking a circular trajectory in cartesian space: The robot was commanded to track a 0.125 Hz circular trajectory in cartesian space with 40 mm amplitude. The reference command was converted to joint references via. inverse kinematics in realtime. Then the modular PID controllers were used to control each joint to follow its reference simultaneously. The tracking errors were within 2 mm. The computer electronics computed all the mathematics within 50 μsec. The tracking control and trajectory planning were used to increase the tracking accuracy (Bouhal *et al*., 1999), especially in this layered manufacturing. The processing system was actually designed to enable highly complex algorithm in the close loop setting.

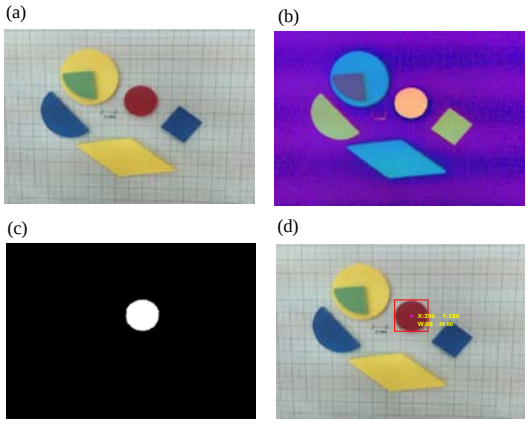

Fig. 4: Visual routine: a) An RGB image taken by the camera; b) The hue image; c) The red feature detected in HSV image and d) The extracted feature

Visual routine: A feature on a primitive product could be detected by color with color based tracking technique (Weijer and Schmid, 2006). A camera normally generated an image in RGB format (Fig. 4a). This RGB image could be converted into HSV color spaces (Fig. 4b). The feature could be easily extracted from this Hue image by specifying the color range of a feature. The resulting image was a black and white image (Fig. 4c). Then blob analysis (Ming and Ma, 2007) was used to determine the object's parameters including the centroid and the bounding box. These parameters were further processed to determine cartesian position of a feature (Fig. 4d).

The cartesian position of a feature relative to the camera was determined using camera projection model. The perspective projection (Hutchinson *et al*., 1996) was used to map the image position (u^n, v^n) in to the cartesian position, ^cX, relative to the camera. The projection model in Fig. 5 showed the relation between the actual position in three dimensional space and its projection in image plane (u^n, v^n). Which Equation π that mapped the image coordinate to the cartesian position is:

$$\pi(x,y,z) = \begin{bmatrix} u^n \\ v^n \end{bmatrix} = \frac{\lambda}{z}\begin{bmatrix} x \\ y \end{bmatrix} \quad (1)$$

Intrinsic parameters of the camera including the focal length λ could be determined using the technique proposed by Zhang (1999) the z-position could be determined if the actual size of a feature was known. As the feature was stationary, the robot was instructed to carry the camera to look at the feature in 4 different views (Fig. 6) the images were then analyzed to find the z-position without a priori known of a feature. Once

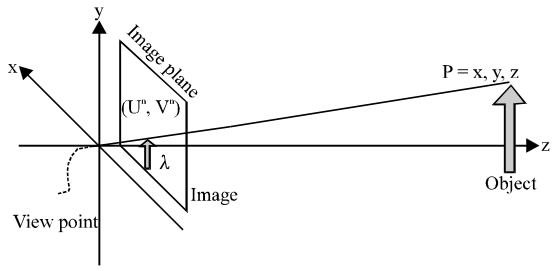

Fig. 5: The projection model

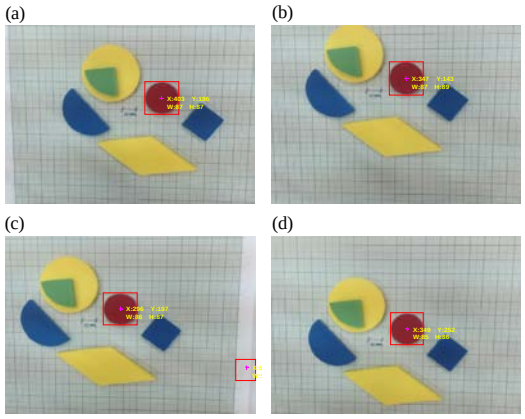

Fig. 6: The red feature in different views, [x y z] = [8.41-11.56 173.36]: a) (15, 0, 0) view point; b) (0, 15, 0) view point; c) (-15, 0, 0) view point and d) (0, -15, 0) view point

the z-position was determined the robot kinematics could be used to determine the z-position in realtime while the x and y-position were determined from (Evans, 2012).

Printed products: In this study, the biopolymer plastic polylactic acid or PLA was used while the primitives were acrylic. Test printing comprised of 3 cases, printing on a flat x-y plane, printing on an inclined surface and centering of a circle on a primitive.

First, the G-code of a thin gear symbol was printed on a flat x-y plane. This printing was used as the baseline comparison with the second case which printed on a 25° inclined plane. The previous G-code of the gear symbol was projected onto the inclined plane with height compensation such that the previously round gear became elongated along the slope and became an oval based shape (Fig. 7a). For both plat surface cases the bonding strength of the features and the primitive seemed to be similar. For the last case a thin cylinder with specified diameter was printed onto a regular base, commercial button magnet holders to show the centering ability of the robot (Fig. 7b).

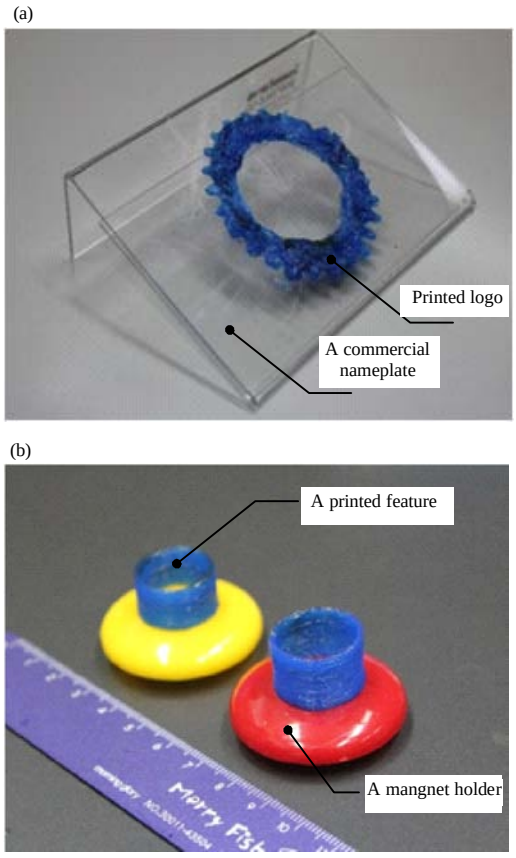

Fig. 7: Some printing results: a) A G-code gear symbol printed on an incline plane and b) A FDM thin cylinder printed on refrigerator magnet holder

RESULTS AND DISCUSSION

During the printing of primitives on top of existing products, there were several points that had been noted as the keys for success. First, the printer head had to be able to be repositioned with respect to the dimension of the primitive object by either manual or visual-based algorithm. In this case, the printing location on the existing primitives could be manually navigated with the aid of an HD camera, installed into the end effector which could determine the build location on the primitives by visual-based algorithm.

Secondly, the printer had to be able to adjust the height in the z-axis of the printing head for good deposition of the crucial first few layers. In this case, the existing primitive product was simply placed on the base with minimal such as drafting tape or no fixtures, depending on the friction between the primitives and the printing surface bed while the robot moved the print head in three-dimensional space over the product to deposit the molten plastic. For primitive products with inclined

surface to be printed on the robot had the ability to probe the inclined plane which was then used to control the height of the print head over the print surface to make sure that the printed first layer was well-aligned to the inclined plane of the primitive surfaced. As the control of a Delta robot was close loop the process could be smoothly executed.

Thirdly, the printed featured had to have satisfactory bonding strength with the primitive base. At present the simply printed PLA products on acrylic were not load bearing structures and could usually be sheared out with no damages to the 3D feature afterwards whether they were tall structures jutting out of the plane with or without rafting or simply thin embossing. For primitives with rough surfaces, the molten plastic would fill in the surface cavities, producing the uneven surfaces that could be easily fitted back onto the primitive.

However, it was expected that the primitive 3D features interface strength could be improved with the proper selection of materials and process parameters. For stop gap the bonding strength could be increased with the additional application of glue or adhesive to the base or across the raft structures. This would be a very simple process as the 3D features had been well positioned on the primitives.

With this process, new features could be added to existing products such that the 3D feature manufacturing, positioning and assembling were combined into a single process. The advantages included the energy, time and cost reductions if the base objects were of simple configuration made from commercial products such as plates or pipes that could be locally bought and easily cut to shape. Then, the 3D features were printed on top with no need for the printing of large base objects beforehand. Moreover, the primitive objects could be functional products that consisted of several assembled components and cheaply available in the mass markets with generally good consideration for sustainable manufacturing (Haapala *et al*., 2013) the printed 3D features would provide the added-on values and individual customization with much less negative impact than the printing of whole substituted parts as well as much less assembling than printing of individual freeform (Sass *et al*., 2005) or embedded elements (Willis *et al*., 2012) that had to be assembled.

With this concept there were many improvement possibilities, ranging from the process itself and the applications. First, the appropriate pairing of base and 3D printed feature materials (Marcincinova and Kuric, 2012) had to be investigated. At present, the simply printed products of the PLA-acrylic were not load bearing structure. While this attribute was not necessary in simple prototypes or embossing, interface strength could be improved with the proper selection of materials and process parameters with measurements (Lee *et al*., 2007) and proper benchmarking with the focus on the first few layers.

If the fused layer thicknesses were controlled and properly varied within the layer by slicer algorithm, the height of 3D feature on inclined plane could be slightly adjusted in each layer and leveled tops could be achieved. In this case, the parameters that affected the quality of finished product such as surface finish (Anitha *et al*., 2001) had to be taken in to account. The positioning of printer head on the primitives for this proposed process could be done manually or with visually-based algorithm. The process could be combined using the collaborative robots or COBOT approach (Peshkin *et al*., 2001) with the aid of a back-drive robot.

As the primitive bases such as plate or other solid shapes, might need some machining beforehand the 3D printing head could be integrated into a reconfigurable machine tools such that the products could be manufacturing from the base object in one continuously process (Perez *et al*., 2014) not to mention the 3D sensing for generating 3D ready-to-print model (Figueroa *et al*., 2013), providing visual aid to the manufacturing of 3D cellular constructs (Yoo, 2014) or even more daring applications to bio-printers (Ho *et al*., 2015) such as the accurate deposition of materials *in vivo*.

CONCLUSION

The highly reconfigurable CHULA DELTA 3D PRINTER R100 incorporated FDM technology into a fast and stiff linear Delta robot with close-loop control such that it could constructed 3D features on top of existing products with 3 main concerns for the final printed quality the repositioned of the printer head the height adjustment of the printer head and the bonding strength between the primitives and the printed features.

Of these three topics, the first 2 involved the performance of the robot/printer. As the resulting accuracy and range of movement could be achieved with the design and selection of components they would be known for each specific assemblage. However, the bonding strength involved the filament quality, primitive materials and operational conditions, specific manufacturing parameters to ensure a sufficient bonding strength for each primitive-feature pairs had to be customized and hence, might be the priority for concern in the wide-scale implementation of the proposed technique.

Despite these concerns the 3D printing of features on commercial products would be a very cost-effective means of adapting existing goods to answer new demands or gain additional functions. It was also another method of product personalization; printed logos and labels, etc. could be easily added to specific manufacturing pieces or batches in the production lines or at distribution locations.

ACKNOWLEDGEMENT

This study was supported by the Chulalongkorn University Strategic Research Grant CU-57-074-AS.

REFERENCES

Alciatore, D.G., 2007. Introduction to Mechatronics and Measurement Systems. Tata McGraw-Hill Education, New York, USA., Pages: 511.

Anitha, R., S. Arunachalam and P. Radhakrishnan, 2001. Critical parameters influencing the quality of prototypes in fused deposition modelling. J. Mater. Process. Technol., 118: 385-388.

Bouhal, A., M.A. Jafari, W.B. Han and T. Fang, 1999. Tracking control and trajectory planning in layered manufacturing applications. IEEE. Trans. Ind. Electron., 46: 445-451.

Cunico, W.M.M. and D.J. Carvalho, 2013. Design of an FDM positioning system and application of an error-cost multiobjective optimization approach. Rapid Prototyping J., 19: 344-352.

Dashchenko, A.I., 2006. Reconfigurable Manufacturing Systems and Transformable Factories. Springer, Berlin, Germany, pp: 111-140.

Dorf, R.C. and R.H. Bishop, 1998. Modern Control Systems. Prentice Hall, New York, USA.,.

Evans, B., 2012. Practical 3D Printers: The Science and Art of 3D Printing. Apress Publishing Company, New York, USA., Pages: 305.

Figueroa, N., H. Dong and E.A. Saddik, 2013. From sense to print: Towards automatic 3D printing from 3D sensing devices. Proceeding of the IEEE International Conference on Systems, Man and Cybernetics, October 13-16, 2013, IEEE, Abu Dhabi, United Arab Emirates, ISBN:978-1-4799-0652-9, pp: 4897-4904.

Haapala, K.R., F. Zhao, J. Camelio, J.W. Sutherland and S.J. Skerlos et al., 2013. A review of engineering research in sustainable manufacturing. J. Manuf. Sci. Eng., 135: 1-16.

Ho, C.M.B., S.H. Ng and Y.J. Yoon, 2015. A review on 3D printed bioimplants. Int. J. Precis. Eng. Manuf., 16: 1035-1046.

Hutchinson, S., G.D. Hager and P.I. Corke, 1996. A tutorial on visual servo control. IEEE Trans. Robot. Automat., 12: 651-670.

Kim, M.S., W.S. Chu, Y.M. Kim, A.P.G. Avila and S.H. Ahn, 2009. Direct metal printing of 3D electrical circuit using rapid prototyping. Int. J. Precis. Eng. Manuf., 10: 147-150.

Lee, C.S., S.G. Kim, H.J. Kim and S.H. Ahn, 2007. Measurement of anisotropic compressive strength of rapid prototyping parts. J. Mater. Process. Technol., 187: 627-630.

Marcincinova, N.L. and I. Kuric, 2012. Basic and advanced materials for fused deposition modeling rapid prototyping technology. Manuf. Ind. Eng., 11: 25-27.

Ming, A. and H. Ma, 2007. A blob detector in color images. Proceedings of the 6th ACM International Conference on Image and Video Retrieval, July 09 -11, 2007, ACM, New York, USA., ISBN:978-1-59593-733-9, pp: 364-370.

Perez, R., A. Molina and R.M. Cadena, 2014. Development of an integrated approach to the design of reconfigurable micro-mesoscale CNC machine tools. J. Manuf. Sci. Eng., 136: 1-10.

Peshkin, M.A., J.E. Colgate, W. Wannasuphoprasit, C.A. Moore and R.B. Gillespie et al., 2001. Cobot architecture. IEEE. Trans. Rob. Autom., 17: 377-390.

Sass, L., K. Shea and M. Powell, 2005. Design production: Constructing freeform designs with rapid prototyping. Digital Des. Quest Paradigms, 1: 261-268.

Weijer, V.D.J. and C. Schmid, 2006. Coloring Local Feature Extraction. In: European Conference on Computer Vision, Leonardis, A., H. Bischof and A. Pinz (Eds.). Springer, Berlin, Germany, ISBN:978-3-540-33834-5, pp: 334-348.

Willis, K., E. Brockmeyer, S. Hudson and I. Poupyrev, 2012. Printed optics: 3D printing of embedded optical elements for interactive devices. Proceedings of the 25th Annual ACM Symposium on user Interface Software and Technology, October 07-10, 2012, ACM, New York, USA., ISBN:978-1-4503-1580-7, pp: 589-598.

Yiu, Y.K., 2002. Geometry, Dynamics and Control of Parallel Manipulators. Ph.D Thesis, Hong Kong University of Science and Technology, Hong Kong.

Yoo, D.J., 2014. Recent trends and challenges in computer-aided design of additive manufacturing-based biomimetic scaffolds and bioartificial organs. Int. J. Precis. Eng. Manuf., 15: 2205-2217.

Zhang, Z., 1999. Flexible camera calibration by viewing a plane from unknown orientations. Proceedings of the 7th IEEE International Conference on Computer Vision, September 20-27, 1999, IEEE, Washington, USA., ISBN:0-7695-0164-8, pp: 666-673.